
This paper was awarded in the III International Competition (1994/95) "First Step to Nobel Prize in Physics" and published in the competition proceedings (*Acta Phys. Pol. A* **89** Supplement, S-35 (1996)). The paper is reproduced here due to kind agreement of the Editorial Board of "Acta Physica Polonica A".

EVOLUTION OF REGULAR AND CHAOTIC MOTIONSO F DOUBLE LINKAGE NONLINEAR MECHANICAL SYSTEM

A. Ovsyannikov

School 145, Kiev, Ukraine

This paper presents the results of a numerical investigation of regular and chaotic motions of a nonlinear dynamical two-well potential system.

PACS numbers: 05.45.+b, 02.30.Jr

1. Introduction

Recently it has been discovered that a nonlinear physical system can degenerate into a chaotic, unpredictable time-development, apparently undistinguishable from random noise, although the system is perfectly deterministic in the sense of being described by well-behaved equations of motion with no stochastic, fluctuating ingredients. Mathematicians and theoretical physicists have made great progress in understanding this transition to chaos (see Ref. [1] and Ref. [2]). Here we will describe such phenomena in the dynamical two-well potential system.

2. Description of the system

Consider a horizontal plane (see Fig. 1) on which a bar is situated. One of the ends of the bar is pinned (without friction) to the plane at a point O so that the end A of the bar can move along the circular trajectory on the plane. Another bar is pinned (without friction) to the bar OA at a point A . These bars are assumed to be rigid and weightless. The masses M and m are attached to the points A and B of the bars respectively. The bar AB and mass m can rotate around the pinning point A with a uniform angular speed. The point A of the system is joined to a fixed point C on the plane by a linear spring and a viscous damper. As may be seen from Fig. 1, when the bar AB does not rotate, there are four static equilibrium positions of the system. Two of these positions are stable when the spring is not deformed. Other two are unstable when the bar AB and the point C on the plane lie along the straight line. Two stable equilibrium positions will be situated in two-well potential. We examine the forced vibration due to rotation of the bar AB .

3. Equation of motion

Let O be the origin of the Cartesian system of coordinates xOy (Fig. 1), L — the length of the bar OA , l — the length of the bar AB , l_1 — the distance between the points

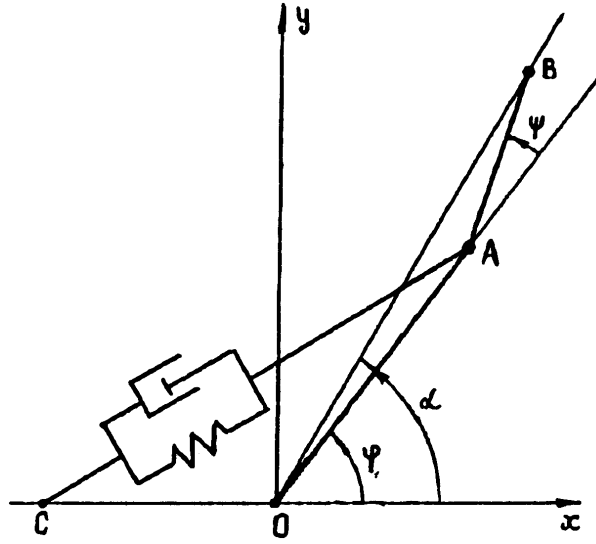


Fig. 1. Investigated system.

O and C , ω — the angular speed of the counterclockwise rotation of the bar AB , φ — the angle formed by the bar OA with respect to the axis x , φ_0 — the initial value of φ ($t = 0$), ψ — the angle formed by bar AB with respect to the line OA , ψ_0 — the initial value of the ψ ($t = 0$), k — the spring's stiffness, γ — the coefficient of viscous damping. In order to obtain the differential Lagrange equation representing the motion of the mechanical system under consideration

$$\frac{d}{dt} \frac{\partial T}{\partial \dot{\varphi}} - \frac{\partial T}{\partial \varphi} + \frac{\partial E}{\partial \varphi} + \frac{\partial D}{\partial \dot{\varphi}} = 0, \quad (1)$$

the total energy of the system has to be expressed in terms of the kinetic energy T , the potential energy E and the dissipative function D .

The kinetic energy T consists of two parts corresponding to the masses M and m

$$T = \frac{M(L\dot{\varphi})^2}{2} + \frac{mV^2}{2}, \quad (2)$$

where V is the velocity of motion of the mass m .

The velocity V consists of velocities of two motions (each for separate bar) and is given by a sum of vector's products

$$\vec{V} = \dot{\vec{\varphi}} \times (\vec{L} + \vec{l}) + \vec{\omega} \times \vec{l} \quad (3)$$

if \vec{h} is radius vector of the mass m and $\vec{h} = \vec{L} + \vec{l}$

$$\vec{V} = \dot{\vec{\varphi}} \times \vec{h} + \vec{\omega} \times (\vec{h} - \vec{L}) \quad (4)$$

then

$$|\vec{V}|^2 = [\dot{\vec{\varphi}} \times \vec{h} + \vec{\omega} \times (\vec{h} - \vec{L})] \times [\dot{\vec{\varphi}} \times \vec{h} + \vec{\omega} \times (\vec{h} - \vec{L})]. \quad (5)$$

Let α be the angle formed by the line OB with respect to the x axis, then the expansions of all vectors in Eq. (4) are

$$\begin{aligned} \dot{\vec{\varphi}} &= 0\vec{i} + 0\vec{j} + \dot{\varphi}\vec{k}, \\ \vec{h} &= |\vec{h}| \cos \alpha \vec{i} + |\vec{h}| \sin \alpha \vec{j} + 0\vec{k}, \end{aligned}$$

$$\begin{aligned}\vec{\omega} &= 0\vec{i} + 0\vec{j} + \omega\vec{k}, \\ \vec{h} - \vec{L} &= l \cos(\omega t + \varphi + \psi_0) + l \sin(\omega t + \varphi + \psi_0) + 0\vec{k}.\end{aligned}\quad (6)$$

Using the equalities

$$\begin{aligned}|\vec{h}| \sin \alpha &= L \sin \varphi + l \sin(\omega t + \psi_0), \\ |\vec{h}| \cos \alpha &= L \cos \varphi + l \cos(\omega t + \psi_0),\end{aligned}$$

one obtains

$$|V|^2 = \dot{\varphi}^2 [L^2 + l^2 + 2Ll \cos(\omega t + \psi_0)] + \omega^2 l^2 + 2\dot{\varphi}\omega l [L \cos(\omega t + \psi_0) + l \cos \varphi].$$

For the kinetic energy of whole system one obtains

$$\begin{aligned}T &= \frac{1}{2}m\{\dot{\varphi}^2 [L^2 + l^2 + 2Ll \cos(\omega t + \psi_0)] + \omega^2 l^2 \\ &\quad + 2\dot{\varphi}\omega l [L \cos(\omega t + \psi_0) + l \cos \varphi]\} + \frac{1}{2}M\dot{\varphi}^2 L^2.\end{aligned}$$

Let us calculate the potential energy of the system now. If l_e is the length of non-deformed spring and l_2 is the length of the deformed spring (when the angle formed by the bar OA with respect to the axis x is φ), then the potential energy is the work or energy stored in the spring during the displacement $l_2 - l_e$. The potential energy of the system is equal to

$$\begin{aligned}U &= \frac{k(l_2 - l_e)^2}{2}, \\ l_2 &= \sqrt{l_1^2 + L^2 + 2l_1L \cos \varphi}, \\ l_e &= \sqrt{l_1^2 + L^2 + 2l_1L \cos \varphi_0},\end{aligned}\quad (7)$$

then

$$U = \frac{k \left(\sqrt{l_1^2 + L^2 + 2l_1L \cos \varphi} - l_e \right)^2}{2}.\quad (8)$$

Reley's dissipative function D is equal to one-half of the coefficient of viscous damping γ times the square of the speed of spring's stretching. Taking into account that the speed is $\frac{d}{dt}(l_2 - l_e)$ for dissipative function one obtains

$$D = \gamma \frac{\left[\frac{d}{dt} \left(\sqrt{l_1^2 + L^2 + 2l_1L \cos \varphi} - l_e \right) \right]^2}{2}\quad (9)$$

or

$$D = \frac{1}{2}\gamma \left(\frac{l_1 L \dot{\varphi} \sin \varphi}{\sqrt{l_1^2 + L^2 + 2l_1L \cos \varphi}} \right)^2.\quad (10)$$

Therefore as the basic energy expressions of the system are known, it is possible to obtain the equation of motion in the form

$$\begin{aligned}& [ML^2 + m(L^2 + l^2) + 2mlL \cos(\omega t + \psi_0)] \frac{d^2\varphi}{dt^2} - 2mLl\omega \sin(\omega t + \psi_0) \frac{d\varphi}{dt} \\ & - m\omega^2 lL \sin(\omega t + \psi_0) + \left(1 - \sqrt{\frac{l_1^2 + L^2 + 2l_1L \cos \varphi_0}{l_1^2 + L^2 + 2l_1L \cos \varphi}} \right) kl_1L \sin \varphi + \gamma \frac{l_1^2 L^2 \dot{\varphi} \sin^2 \varphi}{l_1^2 + L^2 + 2l_1L \cos \varphi} = 0.\end{aligned}\quad (11)$$

Rearranging the terms, using the notation $x = \omega t$ and dividing by $L^2 M \omega^2$ we obtain the following differential equation:

$$\left[1 + \frac{m}{M} \left(1 + \frac{l}{L} \right)^2 + 2 \frac{m l}{M L} \cos(x + \psi_0) \right]^2 \frac{d^2 \varphi}{dx^2} - 2 \frac{m l}{M L} \sin(x + \psi_0) \frac{d\varphi}{dx} - \frac{l_1 \Omega}{L \omega} \left[1 - \sqrt{\frac{1 + \left(\frac{l_1}{L}\right)^2 + 2 \frac{l_1}{L} \cos \varphi_0}{1 + \left(\frac{l_1}{L}\right)^2 + 2 \frac{l_1}{L} \cos \varphi}} \right] - \frac{m l}{M L} \sin(x + \psi_0) + \frac{\gamma}{M \omega} \left(\frac{l_1}{L} \right)^2 \frac{d\varphi}{dx} \frac{\sin^2 \varphi}{1 + \left(\frac{l_1}{L}\right)^2 + 2 \frac{l_1}{L} \cos \varphi} = 0, \quad (12)$$

where $\Omega = \sqrt{k/M}$ is the natural frequency of the spring–mass system. We see that the motion of the system depends on the dimensionless parameters m/M , l/L , l_1/L , Ω/ω , φ_0 , ψ_0 , $\gamma/M\omega$.

4. Numerical analysis and results

For numerical solution of initial value problem for the equation of motion 4th-order Runge–Kutta method is used. As may be seen from the equation, the variable x is in

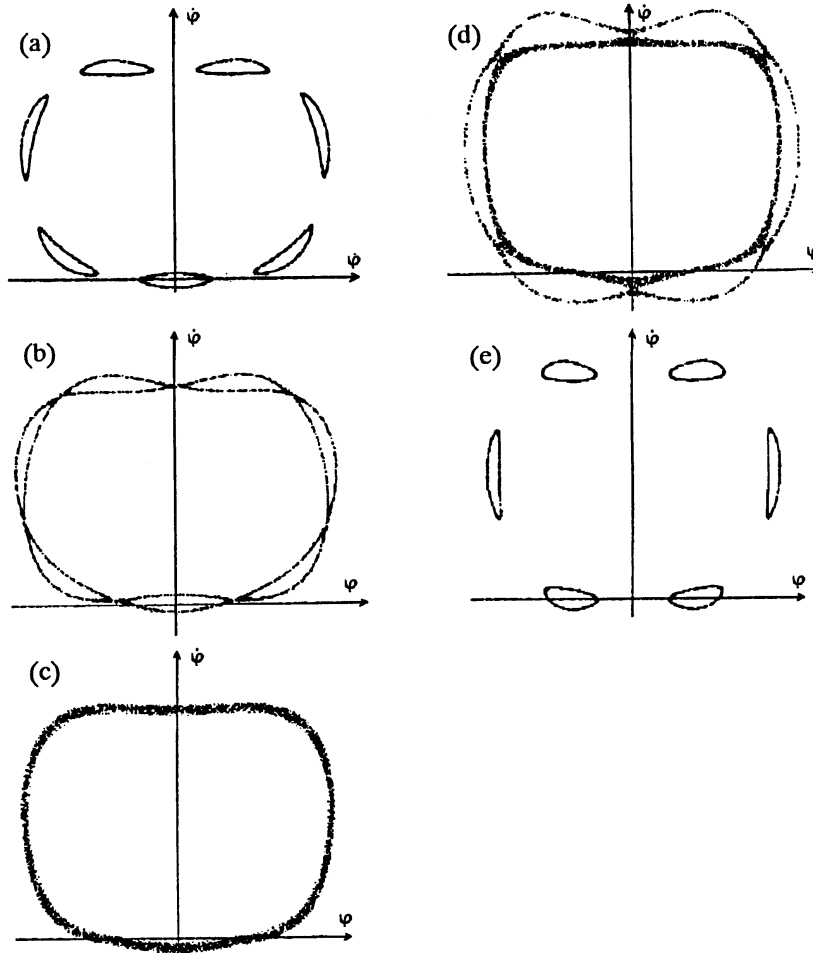


Fig. 2. (a)–(e) Poincaré maps (see text for detail).

interval $[0, 2\pi]$, thereby step size for time integration is taken as $\pi/20$. The stable position of the bar OA is chosen as initial one, i.e.

$$\varphi = \varphi_0 \quad \text{and} \quad \frac{d\varphi}{dx} = 0 \quad \text{for} \quad x = 0.$$

Time integration is stopped when the number of steps reaches 140000.

Let us consider a conservative system for which $\gamma = 0$. This system displays chaotic and quasi-periodic motion (periodic motion has not been found during the numerical experiments). Poincaré maps in Figs. 2a–e show the effect of intermittency (chaotic and quasi-periodic motions change into each other). The Poincaré maps were obtained for the following values of the parameters: $l/L = 0.5$, $m/M = 1.0$, $\Omega/\omega = 1.0$, $\varphi_0 = 20^\circ$, $\psi_0 = 180^\circ$. Values of the ratio l_1/L were 0.2, 0.209, 0.26, 0.3, 0.4 for the cases represented in Figs. 2a–e respectively. The numerical calculation revealed a non-monotonic dependence of system behaviour on the parameter l_1/L . The seven distinct circumferences in the Poincaré map, represented in Fig. 2a, were obtained for the parameter $l_1/L = 0.2$. This is well known case of quasi-periodic motion (Ref. [2]). Initial increase in the parameter, up to the value of 0.26, is accompanied by distinct circumferences in corresponding Poincaré map merge into diffused circumference, see Figs. 2a–c. The width of the circumference obtained for $l_1/L = 0.26$ (Fig. 2c) is at least one order of magnitude greater than the width of the circumference obtained for $l_1/L = 2.2$ (Fig. 2a). Further increase in the parameter drives system back to the quasi-periodic motion, see Figs. 2d,e and 3a. The Poincaré map from Fig. 3a presents circumferences characteristic of quasi-periodic motion similar to that presented in Fig. 2a.

Another intermittency is present in Figs. 3a–c. These Poincaré maps were obtained

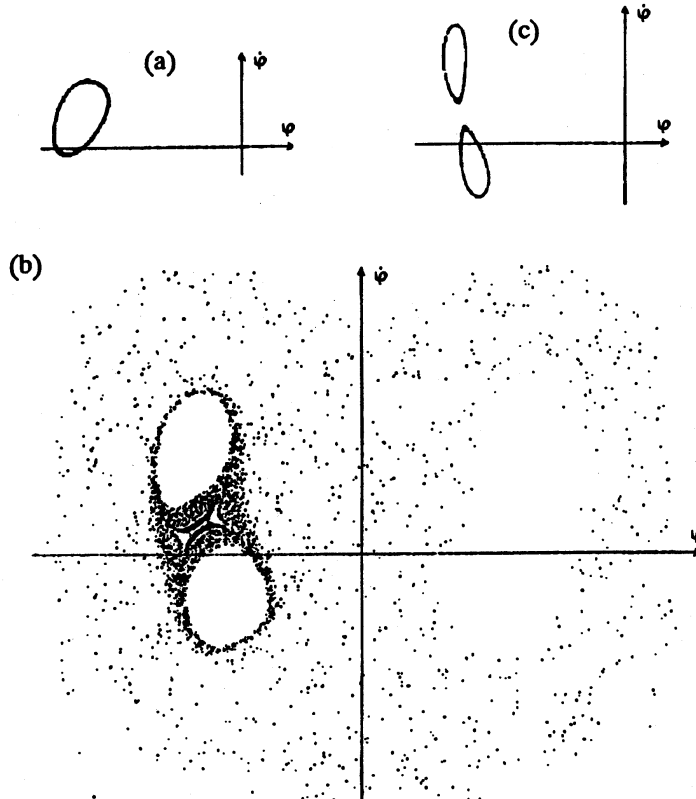


Fig. 3. (a)–(c) Poincaré maps (see text for detail).

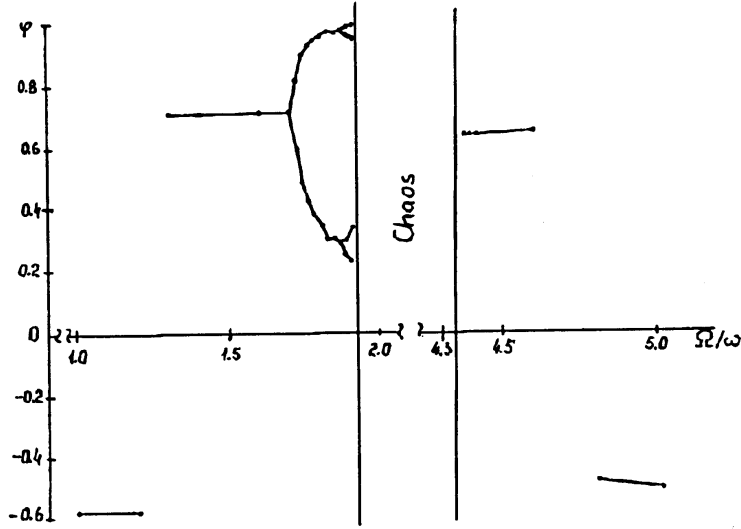


Fig. 4. Bifurcation diagram.

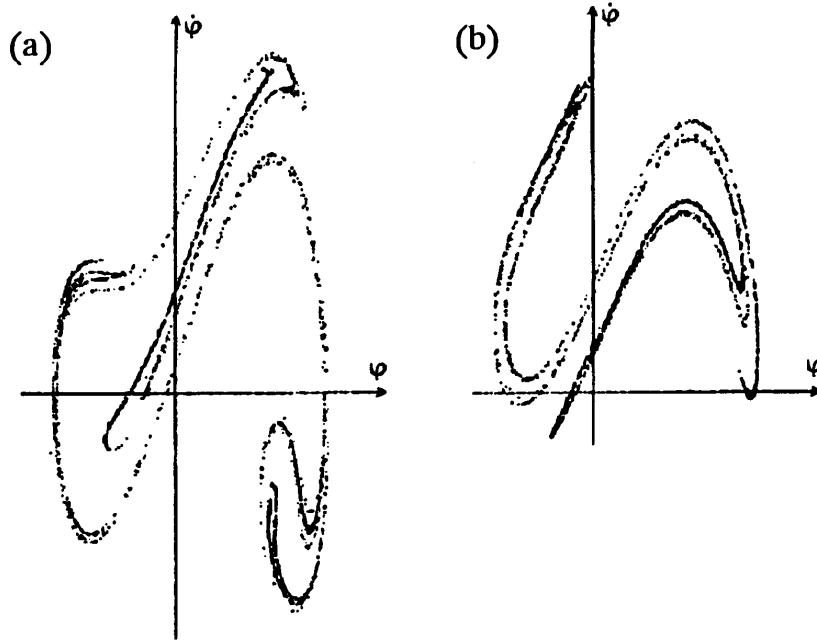


Fig. 5. Chaotic attractor for $\Omega/\omega = 2$ (a) and $\Omega/\omega = 4.3$ (b).

for the following values of parameters:

$$l_1/L = 1.0, m/M = 0.1, \Omega/\omega = 1.0, \varphi_0 = 20^\circ, \psi_0 = 180^\circ.$$

The observed intermittency is due to change of the parameter l/L from 16 through 18 to 20 for Figs. 3a–c, respectively.

Now let us consider the non-conservative system. In the example under consideration the values of parameters were

$$l/L = 2.0, m/M = 0.2, l_1/L = 2.0, \varphi_0 = 20^\circ, \psi_0 = 180^\circ,$$

$$\lambda(l_1/L)^2/M\omega = 10.0.$$

The parameter Ω/ω was chosen as a control parameter. We obtain bifurcation diagram (Fig. 4) showing a cascade of period-doubling and changing the condition of the system.

The unique solution for the value of the control parameter $\Omega/\omega < 1.3$ changes its stability position near $\varphi = -\varphi_0$ and occupies new stability position $\varphi = \varphi_0$. This new unique solution loses its stability at $\Omega/\omega \approx 1.7$. At this value of the control parameter new branches of solution which are stable are generated and so on until a value $\Omega/\omega \approx 1.92$ is reached. In the region of the values of the control parameter $1.92 < \Omega/\omega < 4.33$ the motion of the system is chaotic. When parameter Ω/ω exceeds 4.33, the system occupies the stability position near $\varphi = \varphi_0$ again. At the end when the control parameter $\Omega/\omega > 4.7$, the system occupies stability position near $\varphi = -\varphi_0$. Figures 5a, b represent the chaotic attractor for values $\Omega/\omega = 2.0$ and $\Omega/\omega = 4.3$, respectively.

References

- [1] G.M. Zaslavskiy, *Stokhastichnost dinamicheskikh sistem*, Nauka, Moskva 1984, p. 271
- [2] F. Moon, *Khaoticheskie kolebaniya*, Mir, Moskva 1990, p. 312